The NADPH oxidase NOX2 is a marker of adverse prognosis involved in chemoresistance of acute myeloid leukemias

Rosa Paolillo,[1,2] Mathias Boulanger,[1,2] Pierre Gâtel,[1,2] Ludovic Gabellier,[1,2,3] Marion De Toledo,[1,2] Denis Tempé,[1,2] Rawan Hallal,[1,2] Dana Akl,[1,2] Jérôme Moreaux,[4] Hayeon Baik,[1,2] Elise Gueret,[5] Christian Recher,[6,7] Jean-Emmanuel Sarry,[7] Guillaume Cartron,[3] Marc Piechaczyk[1,2] and Guillaume Bossis[1,2]

[1]IGMM, Univ Montpellier, CNRS, Montpellier; [2]Equipe labellisée Ligue Contre le Cancer, Paris; [3]Département d'Hématologie Clinique, CHU de Montpellier, Montpellier; [4]IGH, Univ Montpellier, CNRS, Montpellier; [5]MGX, Univ Montpellier, CNRS, INSERM, Montpellier; [6]Service d'Hématologie, CHU de Toulouse, Toulouse and [7]CRCT, University of Toulouse, INSERM, CNRS, Toulouse, France

Correspondence: G. Bossis
guillaume.bossis@igmm.cnrs.fr

Received: August 27, 2021.
Accepted: February 8, 2022.
Prepublished: February 17, 2022.

https://doi.org/10.3324/haematol.2021.279889

Supplementary Methods

Pharmacological inhibitors and reagents

Cytosine-β-D-arabinofuranoside (Ara-C), daunorubicin-hydrochloride (DNR) and Phorbol 12-myristate-13-acetate (PMA) were purchased from Sigma-Aldrich. The NADPH oxidase inhibitor VAS2870 was from Enzo Life Sciences. L-012 was from Sobioda (ref W1W120-04891).

Cell culture

HL-60 cell line originates from a patient with AML with maturation (FAB-M2)[1]. U937 is a monocytic cell line originating from a patient with diffuse histiocytic lymphoma[2]. HL-60 and U937 cells were cultured at 37°C in RPMI medium supplemented with 10 % fetal bovine serum (FBS) and streptomycin/penicillin in the presence of 5 % CO_2. Both cell lines were authenticated by the ATCC using Short-Tandem-Repeat analysis. HL-60 and U937 cells resistant to Ara-C and DNR were generated by culturing them in the presence of increasing concentrations of drugs (from 1 nM up to 100 nM for Ara-C and 30 nM for DNR) for 2-3 months[3]. Parental HL-60 cells and resistant HL-60 populations were then cloned using an Aria IIU cell sorter (Becton Dickinson). After amplification, clones were cultured for a maximum of 10 passages.

Cell proliferation and IC_{50} measurement

Cells were seeded at a concentration of $3x10^5$/mL in RPMI medium on day 0 and the number of cells was measured every two-three days using MTS assay (Promega). For IC_{50} measurements, medium was complemented with increasing doses of DNR (Sigma-Aldrich). Viability was measured 24 hours later using MTS assay. IC_{50} were calculated using the GraphPad PRISM software.

NOX activity measurement

$5x10^5$ cells were washed in PBS, resuspended in 100 µL of PBS containing 10 mM glucose and 1mM $CaCl_2$ prewarmed at 37°C and transferred to a white 96-well plate. PMA (100 nM) and VAS2870 (10 µM) were then added to the wells. The luminescent ROS indicator L-012 was then added at a final concentration of 500 µM and luminescence was recorded on a Centro XS^3 LB 960 luminometer (Berthold Technologies).

RT-qPCR assays

Total mRNA was purified using the GenElute Mammalian Total RNA kit (Sigma-Aldrich). After DNase I treatment, 1 µg of total RNA was used for cDNA synthesis using the Maxima First Strand cDNA kit (ThermoFisher Scientific). qPCR assays were conducted using Taq platinum (Invitrogen) and the LightCycler 480 device (Roche) with specific DNA primers (IDT, sequence available on request). Data were normalized to the housekeeping *S26* or *GAPDH* mRNA levels.

RNA-seq mapping, quantification and differential analysis

RNA-seq reads were mapped on the Human reference genome (hg19, GRCh37p13) using TopHat2 (2.1.1)[4] based on the Bowtie2 (2.3.5.1) aligner[5]. The reproducibility of replicates was verified using cufflinks v2.2.1 tool[6] with the linear regression of reads per kilobase per million mapped reads (RPKM) between 2 replicates. Reads association with annotated gene regions was done with the HTseq-count tool v0.11.1[7]. Differential expression analysis was performed with DESeq2[8] using normalization by sequencing depth and parametric negative binomial law to estimate the data dispersion. Genes with a fold change ≥ 2 and an adjusted p-value (FDR) < 0.05 were considered as differentially expressed genes (DEGs).

GSEA, Gene Ontology and co-expression analysis

Ontology analyses were performed using the Panther software[9] (http://www.pantherdb.org/). Gene Set Enrichment Analyses were performed using https://www.gsea-msigdb.org/gsea/index.jsp (version 4.0.3)[10]. Coexpression analyses were performed using the UCSC Xena browser (https://xenabrowser.net/heatmap/) with publicly available data from the Cancer Genome Atlas Program (TCGA)[11].

CRISPR/Cas9 knock-out of CYBB

A control or a *CYBB*-binding Cr-RNA (sequence available on request) was transfected together with a recombinant GFP-Cas9 protein and TracrRNA ATTO 550 (IDT) in HL-60 cells using the Amaxa technology. Twelve hours after transfection, GFP-positive cells were sorted and cloned. The DNA sequence surrounding the targeted CYBB sequence was PCR-amplified on genomic DNA from the selected clones, cloned in the TOPO-TA vector (Life Technologies) and sequenced.

Statistical analyses

Results are presented as means ± S.D of at least 3 biologically-independent experiments. Statistical analyses were performed using the Student t-test or One Way Anova with the

GraphPad Prism software and R.3.6.0 software (R foundation for Statistical Computing, Vienna, Austria). *; **; *** correspond to $P < 0.05$; $P < 0.01$; $P < 0.001$, respectively. ns=not significant. Statistical analyses for the RNA-Seq experiments, GSEA and NOX score are described in the relevant sections.

Supplementary References

1. Dalton Jr WT, Ahearn MJ, McCredie KB, Freireich EJ, Stass SA, Trujillo JM. HL-60 Cell Line Was Derived From a Patient With FAB-M2 and Not FAB-M3. Blood 1988;71(1):242–247.
2. Sundström C, Nilsson K. Establishment and characterization of a human histiocytic lymphoma cell line (U-937). International Journal of Cancer 1976;17(5):565–577.
3. Gâtel P, Brockly F, Reynes C, et al. Ubiquitin and SUMO conjugation as biomarkers of acute myeloid leukemias response to chemotherapies. Life Sci Alliance;3(6):.
4. Kim D, Pertea G, Trapnell C, Pimentel H, Kelley R, Salzberg SL. TopHat2: accurate alignment of transcriptomes in the presence of insertions, deletions and gene fusions. Genome Biol 2013;14(4):R36.
5. Langmead B, Salzberg SL. Fast gapped-read alignment with Bowtie 2. Nat Methods 2012;9(4):357–359.
6. Trapnell C, Roberts A, Goff L, et al. Differential gene and transcript expression analysis of RNA-seq experiments with TopHat and Cufflinks. Nat Protoc 2012;7(3):562–578.
7. Anders S, Pyl PT, Huber W. HTSeq—a Python framework to work with high-throughput sequencing data. Bioinformatics 2015;31(2):166–169.
8. Love MI, Huber W, Anders S. Moderated estimation of fold change and dispersion for RNA-seq data with DESeq2. Genome Biol;15(12):.
9. Mi H, Muruganujan A, Ebert D, Huang X, Thomas PD. PANTHER version 14: more genomes, a new PANTHER GO-slim and improvements in enrichment analysis tools. Nucleic Acids Res 2019;47(D1):D419–D426.
10. Subramanian A, Tamayo P, Mootha VK, et al. Gene set enrichment analysis: A knowledge-based approach for interpreting genome-wide expression profiles. PNAS 2005;102(43):15545–15550.
11. Cancer Genome Atlas Research Network. Genomic and Epigenomic Landscapes of Adult De Novo Acute Myeloid Leukemia. New England Journal of Medicine 2013;368(22):2059–2074.
12. Christopher MJ, Petti AA, Rettig MP, et al. Immune Escape of Relapsed AML Cells after Allogeneic Transplantation. New England Journal of Medicine 2018;379(24):2330–2341.

Supplementary Figures

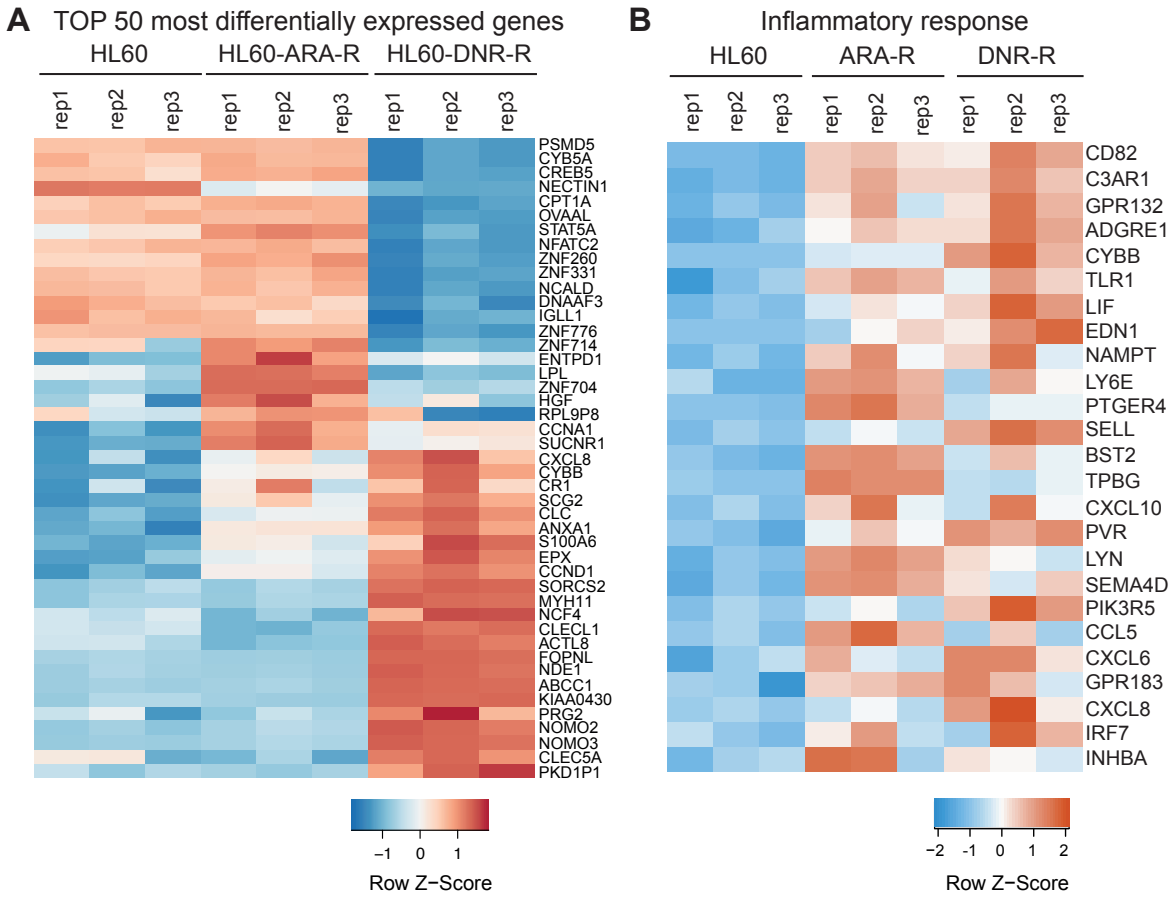

Figure S1: Genes activated in chemoresistant AML cell lines are linked with the inflammatory response. (A) Heatmap for the 50 most differentially expressed genes between parental-, DNR-R- and ARA-R cells. All biological replicates are shown. (B) Heatmap for the top 25 genes from the "inflammatory response" signature in ARA-R, DNR-R and parental HL-60 cells.

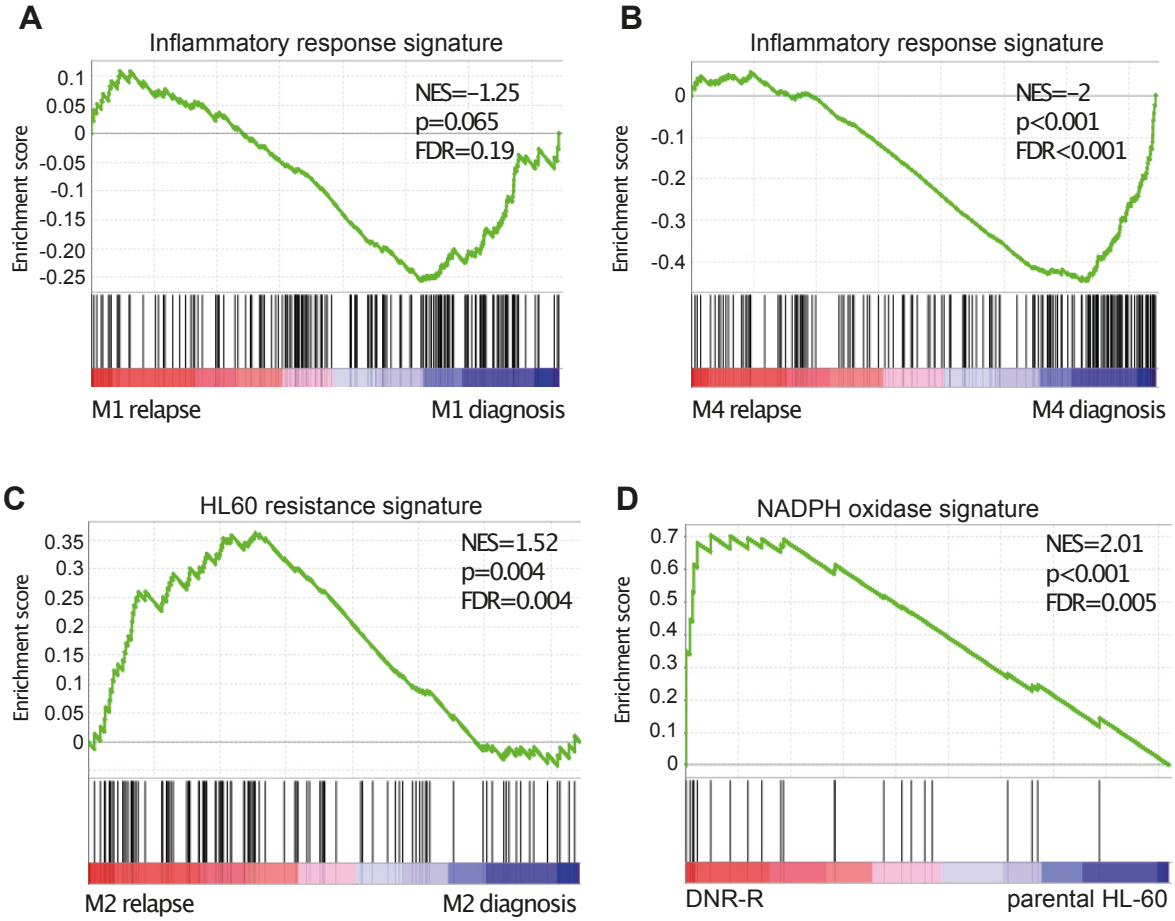

Figure S2. The inflammatory signature is not enriched in FAB M1 and M4 subtypes and a chemoresistance signature is enriched in FAB M2 patients at relapse (A,B) The inflammatory signature (175 genes) was used in GSEA analysis with RNA-Seq data from 3 patients from the FAB M1 (A) or FAB M4 (B) subtype obtained from a publicly available cohort (C) The list of genes induced in both DNR-R and ARA-R compared to parental HL-60 was used in GSEA analysis with RNA-Seq data from 3 patients from the FAB M2 subtype obtained from a publicly available cohort [12]. (D) GSEA was performed using RNA-Seq data from DNR-R and parental HL-60 cells. The enrichment for the "NADPH oxidase" signature (23 genes) is shown. NES (normalized enrichment score), nominal p-value and FDR are presented.

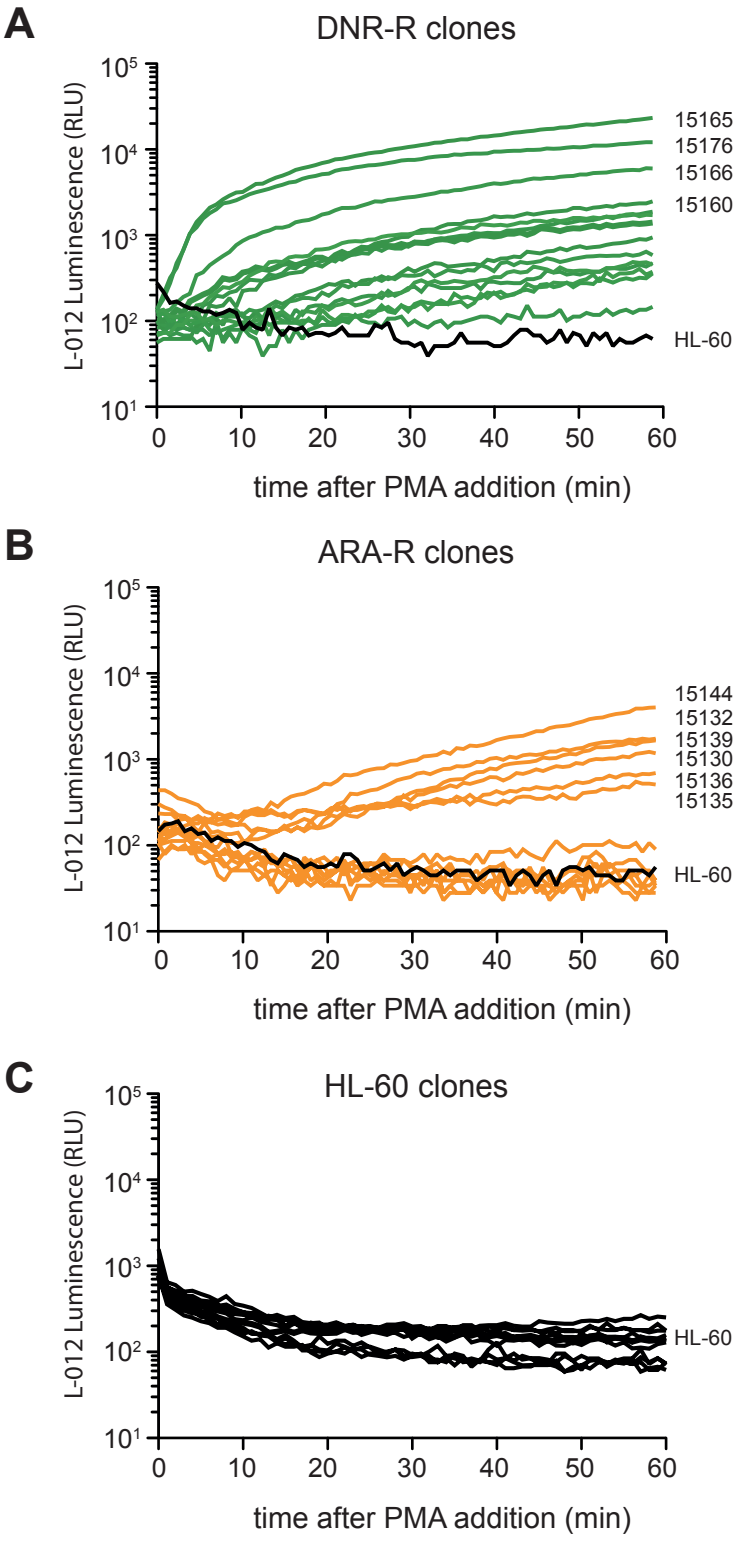

Figure S3: Measurement of NOX2 activity in parental and chemoresistant HL60 clones. ROS production was measured after addition of PMA using L-012 luminescence in (A) DNR-R, (B) ARA-R and (C) HL-60 clones over 1 hr (n=3, a representative experiment is shown).

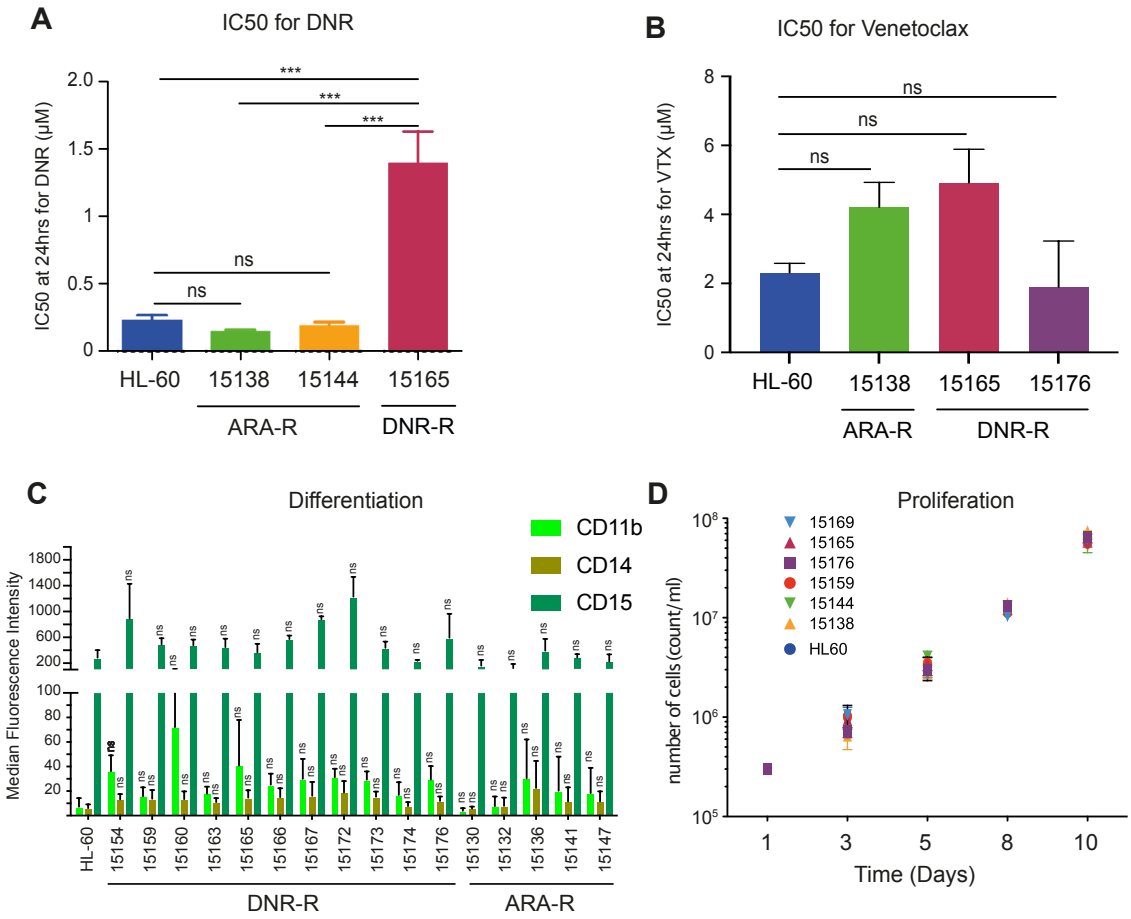

Figure S4: Cross-resistance, proliferation and differentiation of chemoresistant HL-60 clones. (A, B) IC_{50} for DNR (A) or Venetoclax (B) was measured for the indicated cells after 24 hrs of DNR treatment using MTS (n=4 for DNR, n=3 for Venetoclax, mean +/- SD). (C) Parental HL60, DNR-R and ARA-R clones were analyzed by flow cytometry for the expression of CD11b, CD14 and CD15 using CD11b-APC, CD14-PE and CD15-PECy7 antibodies (Miltenyi Biotech). Median Fluorescence Intensities are expressed as ratio to unstained cells (n=3 for CD11b and CD14, n=2 for CD15, mean +/- SD). P-values were calculated using One-way Anova with Dunnett's multiple comparison testing. (D) Cells were seeded at $3x10^5$ on the first day and their proliferation was followed using MTS every 2-3 days for 10 days (n=3, mean +/-SD).

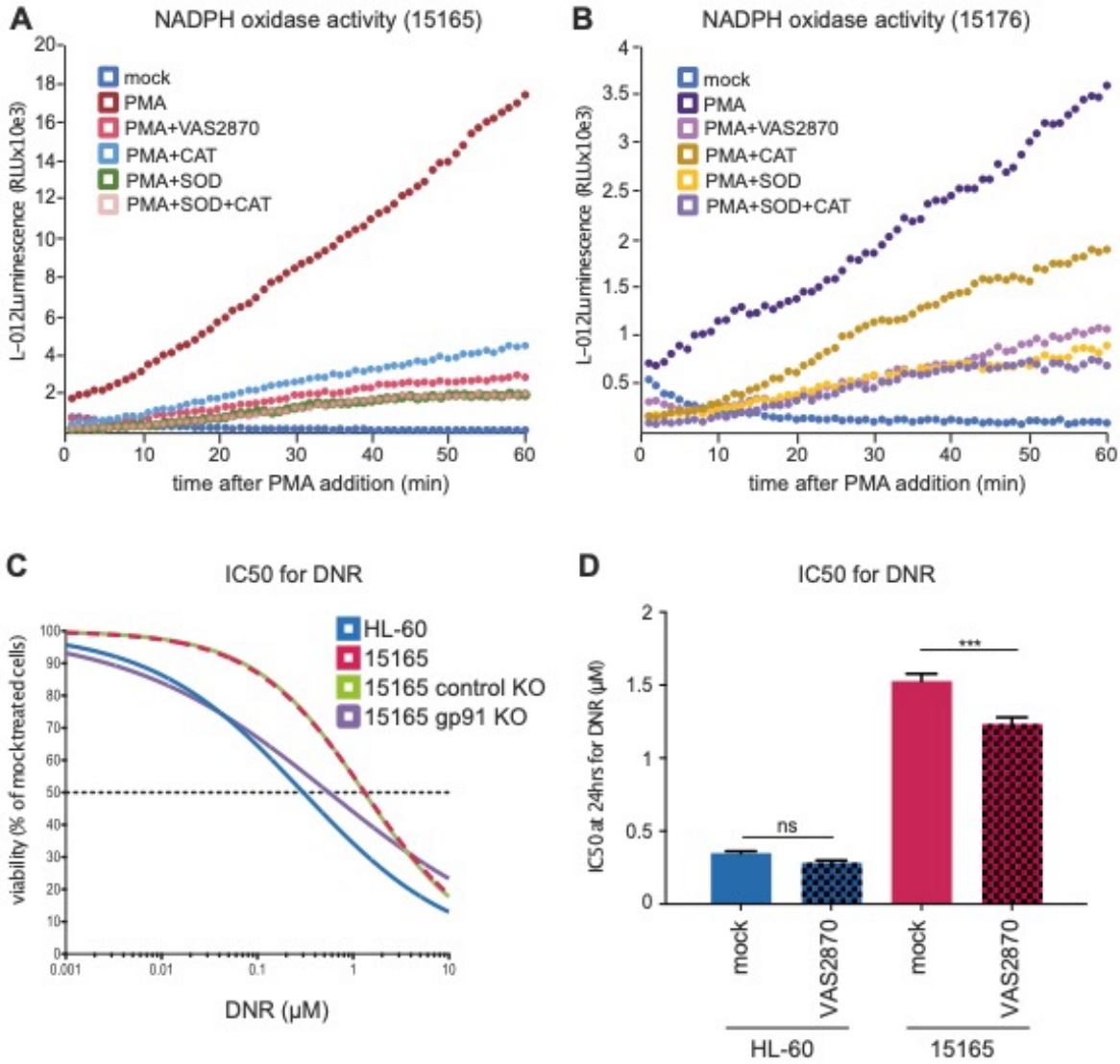

Figure S5. DNR-R clones produce high NOX-derived ROS, which are involved in their resistance to DNR. (A,B) DNR-R clones 15165 (A) and 15176 (B) were stimulated or not with PMA and ROS production was measured by luminometry. When indicated, VAS2870 (10 µM) or SOD (30 U/mL) and/or Catalase (25 µg/mL) were added to the reaction mixture 10 min before PMA addition (n=3, a representative experiment is shown). (C) IC_{50} for DNR was measured after 24 hrs of treatment using MTS (n=4, non-linear fit of all experiments). (D) HL60 and one DNR-R clone (15165) were cultured in the presence of VAS2870 (1µM) for 3 weeks. IC_{50} for DNR was measured after 24 hrs of DNR treatment using MTS (n=4, mean +/- SD). p-values were calculated with One-way Anova and Tukey's multiple comparison test.

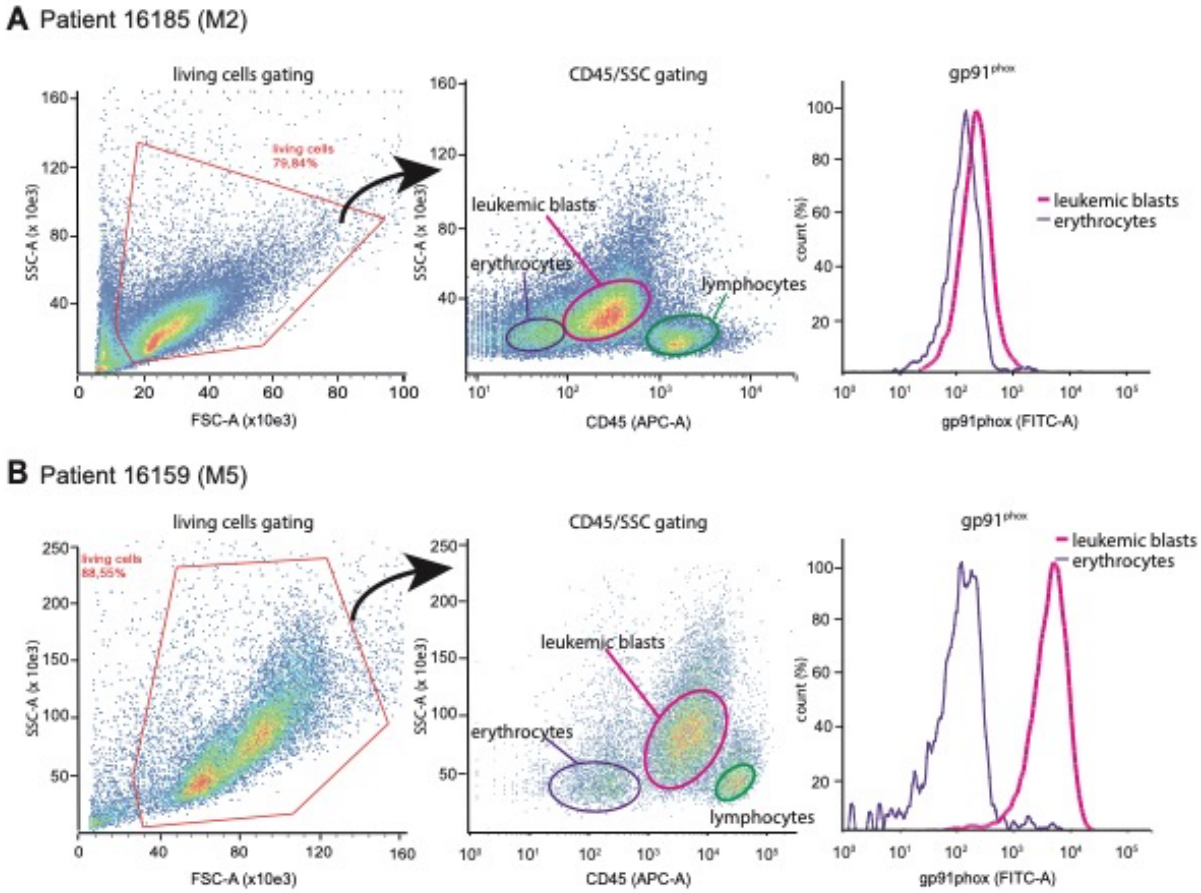

Figure S6: Gating strategy for patient samples. Cells are first distinguished from debris and dead cells using FSC/SSC gating. Using CD45/SSC plot, the leukemic cells are distinguished from other populations present in the sample as $CD45^{dim}/SSC^{low}$. Erythrocytes are $CD45^{neg}/SSC^{low}$ while lymphocytes $CD45^{high}/SSC^{low}$.

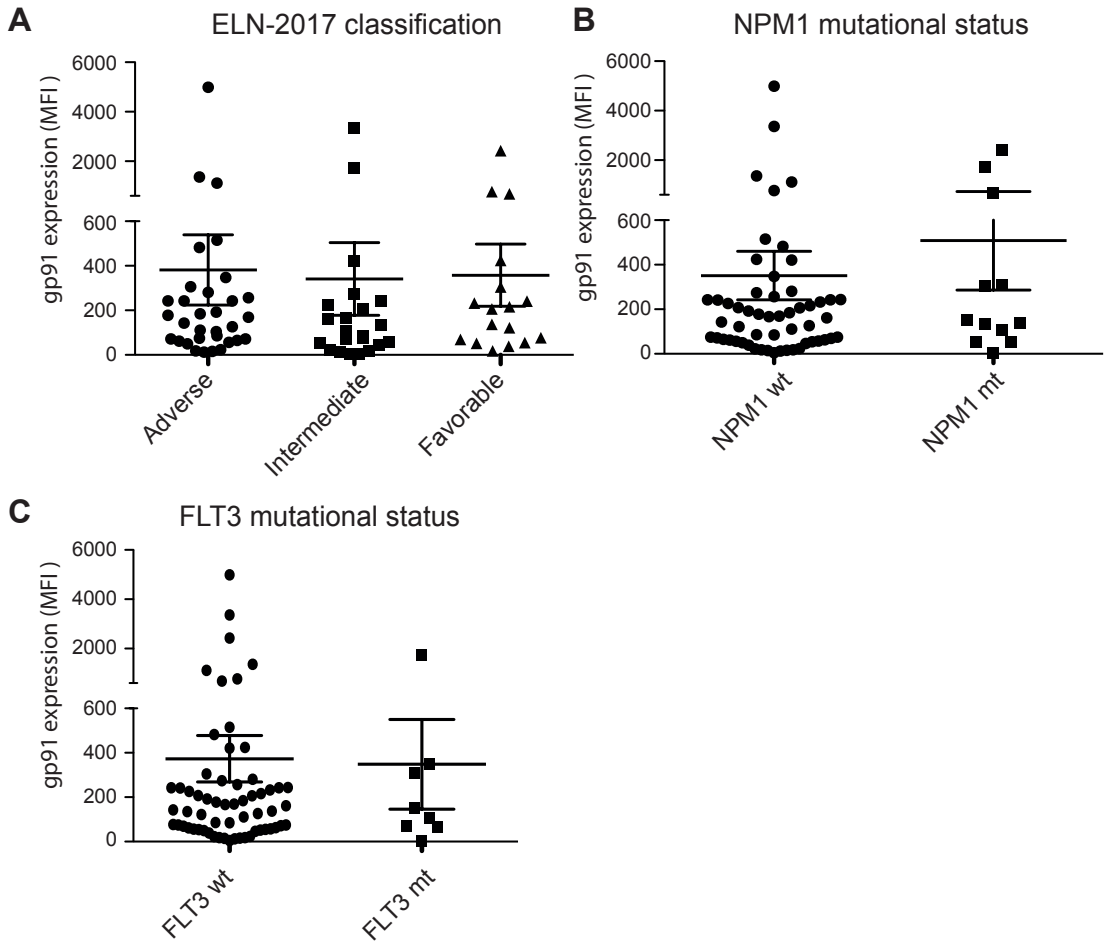

Figure S7: gp91phox expression in AML cells is not correlated with ENL2017 risk classification, NPM1 or FLT3 mutational status. gp91^{phox} expression (MFI) was measured by flow cytometry on bone marrow aspirates from 74 patients taken at diagnosis. Patients are classified according to (A) the ELN-2017 classification, (B) NPM1 mutational status or (C) FLT3 mutational status. No significant differences between groups using Mann-Whitney test.

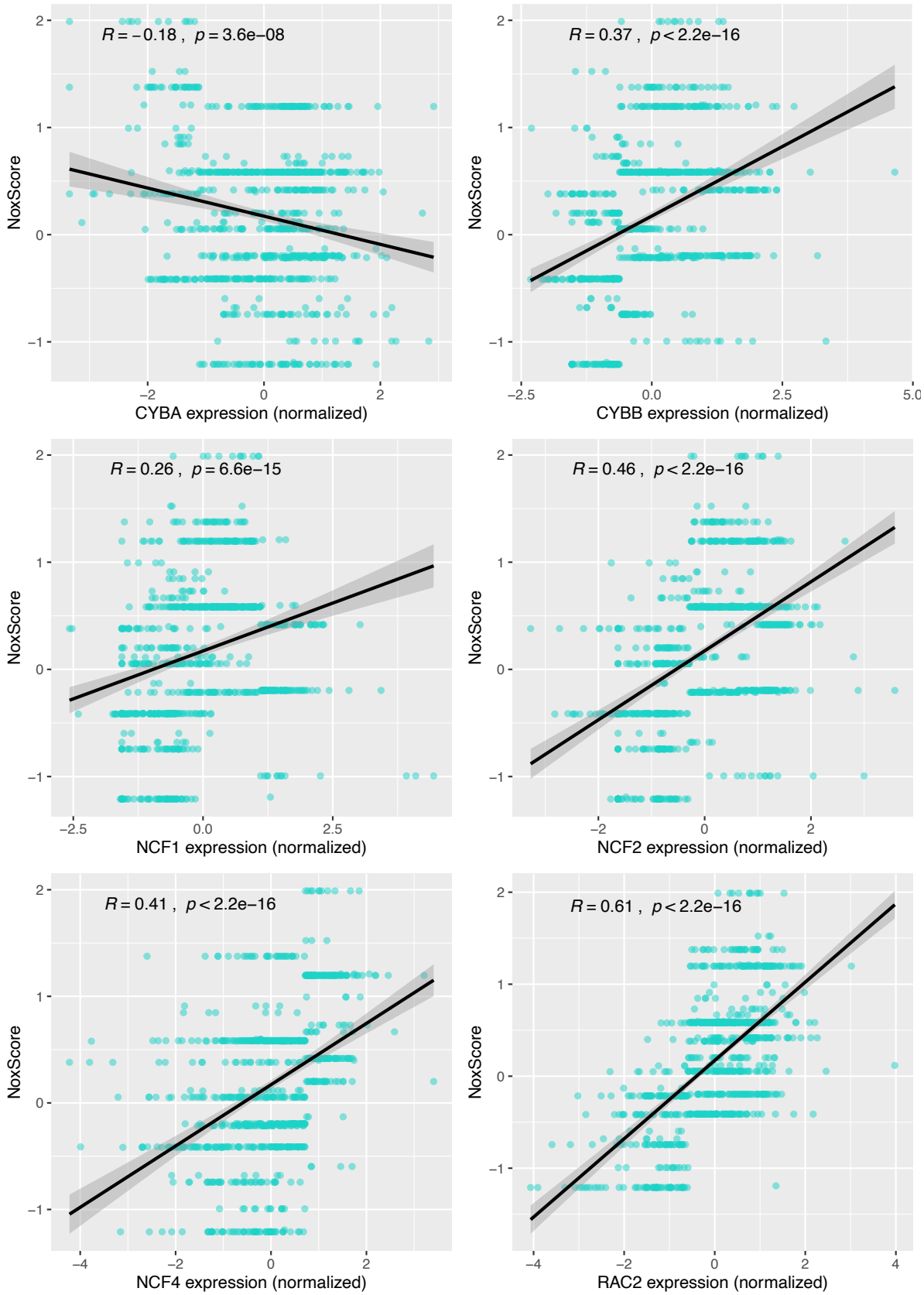

Figure S8: Correlation between the NOX score and the expression of NOX2 genes. The NOX score was plotted as a function of the normalized expression of *CYBA, CYBB, NCF1, NCF2, NCF4* and *RAC2* genes for all patients in the Verhack, Metzeler and TCGA cohorts. Pearson coefficient (R) and associated p-values are indicated.

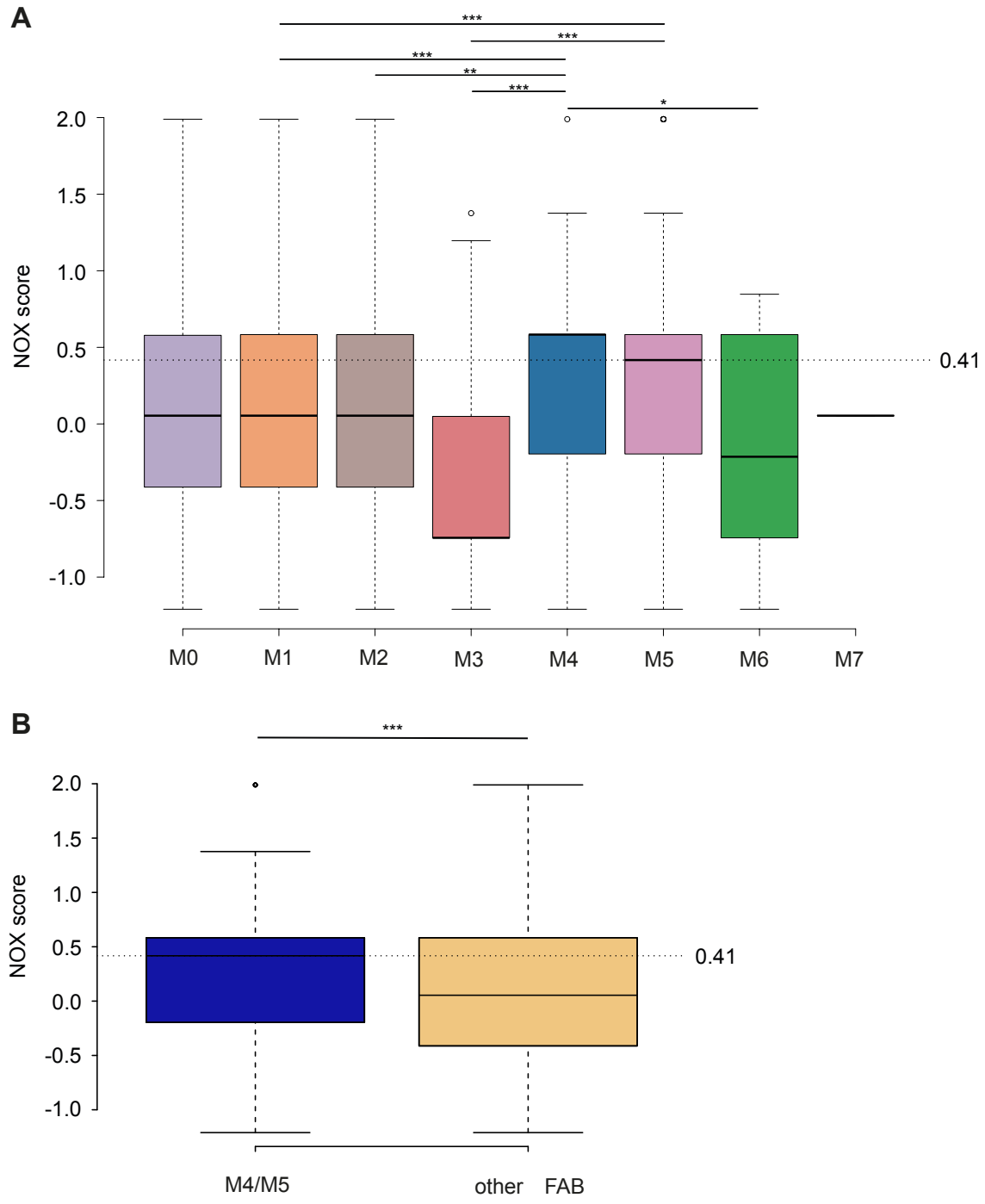

Figure S9: Patients from the FAB M4/M5 subtypes have higher NOX scores. (A) The NOX score was calculated for each FAB subtype using a global cohort comprising all patients from the 3 cohorts (Verhack, Metzeler and TCGA). (B) The NOX score was calculated for M4/M5 and for the other subtypes using the global cohort data. The median NOX scores are indicated as a line and groups were compared using Kruskal-Wallis test (A) and Wilcoxon (B) non parametric tests.

Table S1: Differentially Expressed Genes between DNR-R and ARA-R cells compared to parental HL-60 cells.

Table S2: Ontology analysis of up- and down-regulated genes in DNR-R and ARA-R compared to parental HL-60.

Table S3: Clinical characteristics of the patient included in this study

Table S4: High NOX score gene signature. Mean expression for each Affimetrix probe for all patients from the Verhaak cohort who had a NOX score above 1.37 (10% of patients) was divided by the mean expression for the patients who had a NOX score below 0.41 (50% of patients). The 50 genes having the highest ratio are presented.

Table S5: Prognosis value of the individual NOX genes in the Metzeler cohort. *Gene symbol, adjusted p-value, hazard ratio and prognosis significance are provided for each gene, as determined in the Metzeler cohort (n=240).*

Gene symbol	Hazard ratio	Benjamini Hochberg corrected p-value	Prognosis
CYBA	0,598	0.1013	NS
CYBB	1,479	0.0530	NS
NCF1	0,664	0.0239	Good
NCF2	1,728	0.0397	Poor
NCF4	1,735	0.0122	Poor
RAC2	1,445	0.1050	NS

Table S6: Prognosis value of the individual NOX genes in the TCGA cohort. *Gene symbol, adjusted p-value, hazard ratio and prognosis significance are provided for each gene, as determined in the TCGA cohort (n=148).*

Gene symbol	Hazard ratio	Benjamini Hochberg corrected p-value	Prognosis
CYBA	0,709	0.1107	NS
CYBB	1,281	0.2483	NS
NCF1	2,268	0.0531	NS
NCF2	2,338	0.0048	Poor
NCF4	2,197	0.0047	Poor
RAC2	2,095	0.0009	Poor